Large contribution of fossil-fuel derived secondary organic carbon to water-soluble organic aerosols in winter haze of China

Yan-Lin Zhang[1,2,3*], Imad El-Haddad[3], Ru-Jin Huang[3,4*], Kin-Fai Ho[4,5], Jun-Ji Cao[4*], Yongming Han[4], Peter Zotter[3,#], Carlo Bozzetti[3], Kaspar R. Daellenbach[3], Jay G. Slowik[3], Gary Salazar[2], André S.H. Prévôt[3*], Sönke Szidat[2*]

[1]Yale-NUIST Center on Atmospheric Environment, Nanjing University of Information Science and Technology, 210044 Nanjing, China

[2]Department of Chemistry and Biochemistry & Oeschger Centre for Climate Change Research, University of Bern, 3012 Bern, Switzerland

[3]Paul Scherrer Institute (PSI), 5232 Villigen, Switzerland

[4]Key Laboratory of Aerosol Chemistry and Physics, Institute of Earth Environment, Chinese Academy of Sciences, 710061 Xi'an, China

[5]School of Public Health and Primary Care, The Chinese University of Hong Kong, Hong Kong, China

[*]To whom correspondence should be addressed. E-mail: dryanlinzhang@outlook.com or zhangyanlin@nuist.edu.cn (Y.-L.Z.); andre.prevot@psi.ch (A. Prévôt); rujin.huang@ieecas.cn (R.-J.H.); jjcao@ieecas.cn (J.J.C.); szidat@dcb.unibe.ch (S.S.).

Phone: +86 25 5873 1022; fax: +86 25 5873 1193

Abstract

Water-soluble organic carbon (WSOC) is a large fraction of organic aerosols (OA) globally and has significant impacts on climate and human health. The sources of WSOC remain very uncertain in polluted regions. Here we present a quantitative source apportionment of WSOC isolated from aerosols in China using radiocarbon (^{14}C) and offline high-resolution time-of-flight aerosol mass spectrometer measurements. Fossil emissions on average accounted for 32-47% of WSOC. Secondary organic carbon (SOC) dominated both the non-fossil and fossil derived WSOC, highlighting the importance of secondary formation to WSOC in severe winter haze episodes. Contributions from fossil emissions to SOC were 61±4% and 50±9% in Shanghai and Beijing, respectively, significantly larger than those in Guangzhou (36±9%) and Xi'an (26±9%). The most important primary sources were biomass burning emissions, contributing 17-26% of WSOC. The remaining primary sources such as coal combustion, cooking and traffic were generally very small but not negligible contributors, as coal combustion contribution could exceed 10%. Taken together with earlier ^{14}C source apportionment studies in urban, rural, semi-urban, and background regions in Asia, Europe and USA, we demonstrated a dominant contribution of non-fossil emissions (i.e., 75±11%) to WSOC aerosols in the North Hemisphere; however, the fossil fraction is substantially larger in aerosols from East Asia and the East Asian pollution outflow especially during winter due to increasing coal combustion. Inclusion of our findings can improve a modelling of effects of WSOC aerosols on climate, atmospheric chemistry and public health.

1 INTRODUCTION

Water-soluble organic carbon (WSOC) is a large fraction of atmospheric organic aerosols (OA), which contributes approximately 10% to 80% of the total mass of organic carbon (OC) in aerosols from urban, rural and remote sites (Zappoli et al., 1999;Weber et al., 2007;Ruellan and Cachier, 2001;Wozniak et al., 2012;Mayol-Bracero et al., 2002). Only 10 to 20% of total mass of WSOC has been resolved at a molecular level, and it consists of a large variety of chemical species such as mono- and di-carboxylic acids, carbohydrate derivatives, alcohols, aliphatic and aromatic acids and amino acids (Fu et al., 2015;Noziere et al., 2015). Recent studies suggest that the water-soluble fraction of HUmic LIke Substances (HULIS) is a major component of WSOC, which exhibits light-absorbing properties (Limbeck et al., 2005;Andreae and Gelencser, 2006;Laskin et al., 2015). Therefore, WSOC has significant influences on the Earth's climate either directly by scattering and absorbing radiation or indirectly by altering the hygroscopic properties of aerosols and increasing cloud condensation nuclei (CCN) activity (Asa-Awuku et al., 2011;Cheng et al., 2011;Hecobian et al., 2010).

WSOC can be directly emitted as primary particles mainly from biomass burning emissions or produced from secondary organic aerosol (SOA) formation (Sannigrahi et al., 2006;Kondo et al., 2007;Weber et al., 2007;Bozzetti et al., 2017b;Bozzetti et al., 2017a). Ambient studies provide evidence that SOA formation through the oxidation of volatile organic compounds (VOCs) and gas-to-particle conversion processes may be a prevalent source of WSOC (Kondo et al., 2007;Weber et al., 2007;Miyazaki et al., 2006;Hecobian et al., 2010). WSOC is therefore thought to be a good proxy of secondary organic carbon (SOC) in the absence of biomass burning (Weber et al., 2007). By contrast, water-insoluble OC (WIOC) is thought to be mainly from primary origins with a substantial contribution from fossil fuel emissions (Miyazaki et al., 2006;Zhang et al., 2014b).

Due to a large variety of sources and unresolved formation processes of WSOC, their relative fossil and non-fossil contributions are still poorly constrained. Radiocarbon (^{14}C) analysis of sub-fractions of organic aerosols such as OC, WIOC and WSOC enable an

unambiguous, precise and quantitative determination of their fossil and non-fossil sources (Zhang et al., 2012;Zhang et al., 2014b;Zhang et al., 2014c;Zong et al., 2016;Cao et al., 2017). Meanwhile, the application of aerosol mass spectrometer measurement and positive matrix factorization and multi-linear engine 2 (ME-2) can quantitatively classify organic aerosols into two major types such as hydrocarbon-like OA (HOA) from primary fossil-fuel combustion and oxygenated organic aerosol (OOA) from secondary origin (Zhang et al., 2007;Jimenez et al., 2009). Field campaigns with the aerosol mass spectrometer (AMS) have revealed a predominance of OOA in various atmospheric environments, although their sources remain poorly characterized (Zhang et al., 2007;Jimenez et al., 2009). Previous studies found OOA is strongly correlated with WSOC from urban aerosols in Tokyo, Japan, the Pearl River Delta (PRD) in South China and Helsinki, Finland, indicating similar chemical characteristics, sources and formation processes of OOA and WSOC (Kondo et al., 2007;Xiao et al., 2011;Timonen et al., 2013). Similarly, HOA is mostly water insoluble and the major portion of water insoluble OC (WIOC) can be assigned as HOA (Kondo et al., 2007;Daellenbach et al., 2016). Therefore, ^{14}C measurement of WIOC and WSOC aerosols may provide new insights into sources and formation processes of primary and secondary OA, respectively, which also will elucidate the origin of HOA and OOA as measured by AMS (Zotter et al., 2014b;Zhang et al., 2017).

In this paper we apply a newly developed method to measure ^{14}C in WSOC of $PM_{2.5}$ (particulate matter with an aerodynamic diameter of small than 2.5 μm) samples collected at four Chinese megacities during an extremely severe haze episode during winter 2013 (Zhang et al., 2015b;Huang et al., 2014). In conjunction with our previous dataset from the same campaign, we quantify fossil and non-fossil emissions from primary and secondary sources of WSOC and WIOC. The dataset is also complemented by previous ^{14}C-based source apportionment studies conducted in urban, rural and remote regions in the North Hemisphere to gain an overall picture of the sources of WSOC aerosols.

2 MATERIALS AND METHODS

2.1 Sampling

During January 2013 extremely high concentrations of 24-h $PM_{2.5}$ (i.e. often >100 μg/m^3) were identified in several large cities in East China (Huang et al., 2014;Zhang et al., 2015b). To investigate sources and formation mechanisms of the haze particles, an intensive field campaign was carried out in four large cities, Beijing, Xi'an, Shanghai and Guangzhou, which are representative cities of the Beijing-Tianjin-Hebei region, central-northwest region, Yangtze Delta Region, and Pearl River Delta Region, respectively. The sampling procedures have been previously described in detail elsewhere (Zhang et al., 2015b). Briefly, $PM_{2.5}$ samples were collected on pre-baked (450 °C for 6 hours) quartz filters using high-volume samplers for 24 h at a flow rate of ~1.05 m^3/min from 5 to 25 January 2013. The sampling sites in each city were located at campuses of universities or at research institutes, at least 100 m away from major emission sources (e.g., roadways, industry and domestic sources). One field blank sample for each site was collected and analyzed. The results reported here were corrected for these field blanks (Zotter et al., 2014a;Cao et al., 2013). All samples were stored at -20 °C before analysis. The $PM_{2.5}$ mass was gravimetrically measured with an analytical microbalance before and after sampling with the same conditions (~12 hour)

2.2 OC and EC mass determinations

A 1.0 cm^2 filter punches were used for OC and EC mass determination with a OC/EC analyzer (Model4L) using the EUSAAR_2 protocol (Cavalli et al., 2010). The replicate analysis (n=6) showed an analytical precision with relative standard deviations smaller than 5%, 10%, and 5% for OC, EC and TC, respectively. The field blank of OC was on average 2.0 ± 1.0 μg/cm^2 (equivalent to ~0.5 μg/m^3), which was used for blank correction for OC. EC data was not corrected for field blank, because such a blank was not detectable.

2.3 Offline-AMS measurement and PMF source apportionment

The water-soluble extracts from the same samples were analyzed by a high-resolution time of flight aerosol mass spectrometer (HR-ToF-AMS) and the resulting mass spectra were used as

an inputs for positive matrix factorization (PMF) for the source apportionment of the WSOC, OC and $PM_{2.5}$. The methodology applied, and the AMS-PMF results obtained are detailed in Huang et al. (2014) and will only be briefly described in the following. Here, only data relative to WSOC are used.

Filter punches (the equivalent of ~4 cm^2) were sonicated in 10 mL ultrapure water (18.2 MΩ cm at 25 °C, TOC <3ppb) for 20 min at 30°C. The water extracts were aerosolized and the resulting particles were dried with a silica gel diffusion dryer before analysis by the HR-ToF-AMS. For each measurement ten mass spectra were recorded (AMS V-mode, m/z 12-500), with a collection time for each spectrum of 1 minute.

Online AMS measurements provide quantitative mass spectra of submicron non-refractory aerosol species, including organic aerosol and ammonium nitrate and sulfate. However, the offline AMS measurements described herein cannot be directly related to ambient concentrations due to uncertainties in nebulization and AMS lens cut-off. Here, we have scaled the organic aerosol mass spectra to water soluble organic aerosol concentrations (WSOM), obtained as WSOC times OM/OC ratios. The latter were determined by the high resolution analysis of the organic aerosol mass spectra, acquired by the AMS.

The quantitative WSOM mass spectra are used together with other aerosol species (listed below), collectively referred to as 'species' hereafter, as PMF inputs. PMF solves the bilinear matrix equation:

$$\boldsymbol{X_{ij}} = \sum_{\boldsymbol{k}} \boldsymbol{G_{i,k}} \boldsymbol{F_{k,j}} + \boldsymbol{E_{i,j}} \qquad \text{(Eq. 1)}$$

by following a weighted least squares approach. In the equation, $\boldsymbol{i}$ represent the time index, $\boldsymbol{j}$ a species and $\boldsymbol{k}$ the factor number. $\boldsymbol{X_{ij}}$ is the input matrix, $\boldsymbol{G_{i,k}}$ is the matrix of the factor time-series, $\boldsymbol{F_{k,j}}$ is the matrix of the factor profiles and $\boldsymbol{E_{i,j}}$ the model residual matrix. PMF determines $\boldsymbol{G_{i,k}}$ and $\boldsymbol{F_{k,j}}$ such that the ratio of the Frobenius norm of $\boldsymbol{E_{i,j}}$ over the uncertainty matrix, $\boldsymbol{s_{i,j}}$, used as model input is minimised.

144 The species considered as inputs include the quantitative WSOM mass spectra, organic markers
145 (3 anhydrous sugars, 4 lignin breakdown products, 2 resin acids, 4 hopanes, 19 polycyclic
146 aromatic hydrocarbons and their oxygenated derivatives), EC, and major ions (Cl^-, NO_3^-, SO_4^{2-},
147 oxalate, methylsulfonic acid, Na^+, K^+, Mg^{2+}, Ca^{2+}, and NH_4^+) and residual PM. The latter is the
148 difference between total $PM_{2.5}$ mass and the measured species. It represents our best estimate
149 of the particulate chemical species not measured here, most likely dominated by crustal material.

150 The Source Finder toolkit (SoFi v.4.9) (Canonaco et al., 2013) for IGOR Pro software package
151 (Wavemetrics, Inc., Portland, OR, USA) was used to run the PMF algorithm. The PMF was
152 solved by the Multilinear Engine 2 (ME-2, Paatero, 1999), which allows the constraining of the
153 $\boldsymbol{F_{k,j}}$ elements to vary within a certain range defined by the scalar α ($0 \leq \alpha \leq 1$), such that the
154 modelled $\boldsymbol{F'_{k,j}}$ equals:

155 $$\boldsymbol{F'_{k,j}} = \boldsymbol{F_{k,j}} \pm \alpha * \boldsymbol{F_{k,j}} \quad \text{(Eq. 2)}$$

156 The elements that were constrained in $\boldsymbol{F_{k,j}}$ matrix can be found in Huang et al. (2014). The
157 factors extracted by ME-2 were interpreted to be related to primary emissions from traffic (TR),
158 biomass burning (BB), coal burning (CC), cooking emissions (CI) and dust and from two
159 secondary aerosol fractions. The contributions of the water soluble organic aerosol related to
160 these different factors were determined by the multiplying their relative abundance in the factor
161 profiles by the respective factor time-series. The factors WSOM time series were then divided
162 by the respective OM/OC_k calculated from the high-resolution analysis of the factor mass
163 spectral profile to obtain the $WSOC_k$ time series related to each of the factors. The average
164 OM/OC_k are: 1.25, 1.39, 1.49, 1.55, 2.25, and 2.4 for TR, CI, BB, CB, SOA, and dust,
165 respectively. In the following analysis, the mass of $WSOC_k$ related to coal burning and traffic
166 were assigned to fossil WSOC fraction, while the mass of $WSOC_k$ related to biomass burning
167 and cooking emissions were assigned to non-fossil WSOC fraction (see Sec. 2.5). Meanwhile,
168 the remaining WSOC fractions are assigned to the secondary factors, which can be from both

fossil and non-fossil origins, were considered collectively and compared to the unassigned fossil and non-fossil WSOC, to retrieve the origins of this remaining fraction (see Sec. 2.5).

2.4 ^{14}C measurement of WSOC

^{14}C content of micro-scale WSOC aerosol samples was measured with a newly developed method (Zhang et al., 2014c). Briefly, a 16-mm-diameter punch of each filter was extracted using 10 ml ultrapure water with low TOC impurity (less than 5 ppb). The water extracts were recovered in the 20 ml PFA vials and were then pre-frozen at -20 °C more than 5 hours before completely dryness in a freeze dryer (Alpha 2-4 LSC, Christ, Germany) for about 24 h to 36 h. The residue was re-dissolved in 50 µl of ultrapure water three times and transferred into 200 µl tin capsules (Elementar, Germany). The concentrated samples were heated in the oven at 55-60 °C until complete dryness before the ^{14}C measurements.

WSOC extracts in tin capsules were then converted to CO_2 by the oxidation of the carbon-containing samples using an Elemental Analyzer (EA, Model Vario Micro, Elementar, Germany) as a combustion unit (up to 1050 °C). The resulting CO_2 was introduced continuously by a versatile gas inlet system into a gas ion source of the accelerator mass spectrometer MICADAS where ^{14}C of CO_2 was finally measured (Wacker et al., 2013;Salazar et al., 2015). The ^{14}C content of OC and EC was measured in our previous study (Zhang et al., 2015b). ^{14}C results were expressed as fraction of modern (f_M), i.e., the fraction of the measured $^{14}C/^{12}C$ ratio related to the $^{14}C/^{12}C$ ratio of the reference year 1950 (Stuiver, 1977). To correct excess ^{14}C from nuclear bomb tests in the 1950s and 1960s, f_M values were converted to the fraction of non-fossil (f_{NF}) (Zotter et al., 2014a;Zhang et al., 2012):

$$f_{NF}=f_M/f_{M,ref} \quad \text{(Eq. 3)}$$

$f_{M,ref}$ is a reference value of f_M for non-fossil carbon sources including biogenic and biomass burning emissions, which were estimated as 1.08±0.05 (i.e., $f_{M,ref}$=(0.5*1.10+0.5*1.05)

(see details in (Zhang et al., 2012)) for WSOC samples collected in 2013 according to the contemporary atmospheric CO_2 f_M (Levin et al., 2010) and a tree growth model (Mohn et al., 2008).

2.5 AMS^2-based source apportionment of WSOC

To better understand the origin of WSOC observed at these sites, WSOC sources were apportioned into several major sources by a combination of ^{14}C and PMF source apportionments (See Figure 1). Here, two "AMS" (i.e., accelerator mass spectrometer and aerosol mass spectrometer), such a combined approach was named as "AMS^2-based source apportionment.

WSOC concentration from non-fossil ($WSOC_{NF}$) and fossil ($WSOC_F$) sources were calculated from:

$$WSOC_{NF}=WSOC*f_{NF}(WSOC) \quad \text{(Eq. 4)}$$

$$WSOC_F=WSOC-WSOC_{NF} \quad \text{(Eq. 5)}$$

The mass concentration of WSOC was derived from the subtraction of TC mass measured from a water-extracted filter from that measured with an un-treated filter (Zhang et al., 2012):

$$WSOC=TC_{un\text{-}treated}-TC_{water\text{-}extracted} \quad \text{(Eq.6)}$$

Based on mass balance, WIOC concentrations from non-fossil ($WIOC_{NF}$) and fossil ($WIOC_F$) sources were calculated from:

$$WIOC_{NF}=OC_{NF}-WSOC_{NF} \quad \text{(Eq. 7)}$$

$$WIOC_F=OC_F-WSOC_F \quad \text{(Eq.8)}$$

where OC concentrations from non-fossil (OC_{NF}) and fossil (OC_F) sources were obtained by mass and ^{14}C measurement of the OC fraction, which were reported previously (Zhang et al., 2015b).

The non-fossil and fossil-fuel derived WSOC can be apportioned into primary and secondary OC:

$$WSOC_{NF}=WSOC_{POC,NF}+WSOC_{SOC,NF} \quad (Eq.9)$$

$$WSOC_F= WSOC_{POC,F}+WSOC_{SOC,F} \quad (Eq.10)$$

$WSOC_{POC,NF}$ can be sub-divided into the following three major primary emissions including cooking emission ($WSOC_{CI}$) and biomass burning ($WSOC_{BB}$).

$$WSOC_{POC,NF}=WSOC_{CI}+WSOC_{BB} \quad (Eq.11)$$

Similarly, $WSOC_{POC,F}$ can be sub-divided into the following two major primary emissions including traffic ($WSOC_{TR}$) and coal combustion ($WSOC_{CB}$).

$$WSOC_{POC,F}=WSOC_{TR}+WSOC_{CB} \quad (Eq.12)$$

where primary fractions such as $WSOC_{CI}$, $WSOC_{BB}$, $WSOC_{TR}$ and $WSOC_{CB}$ are previously estimated by the off-line AMS-PMF approach (Huang et al., 2014;Daellenbach et al., 2016;Bozzetti et al., 2017a;Bozzetti et al., 2017b).

An uncertainty propagation scheme using a Latin-hypercube sampling (LHS) model was implemented to properly estimate overall uncertainties including measurement uncertainties of the mass determinations of carbon species (i.e., OC, EC, TC, WSOC, WIOC) and ^{14}C measurement, blank corrections from field blanks, and estimation of $f_{M,ref}$ (Zhang et al., 2015b).

3 RESULTS AND DISCUSSION

3.1 Overall results

During the haze periods of January 2013, the highest daily average $PM_{2.5}$ concentrations were found in Xi'an (345 μg/m^3) followed by Beijing (158 μg/m^3), Shanghai (90 μg/m^3) and Guangzhou (68 μg/m^3). These levels were much higher than the China's National ambient Air quality standards (i.e., 35 μg/m^3). Indeed, several studies have already reported the chemical composition, source and formation mechanism of $PM_{2.5}$ in many large cities during the haze events of January 2013 in East China. For examples, Huang et al. (2014) revealed that the secondary aerosol formation contributed to 44–71% of OA in Beijing, Xi'an, Shanghai, and Guangzhou during this extremely haze event in China (Huang et al., 2014). By ^{14}C-based source appointment conducted in the same campaign, Zhang et al. (2015) have reported that carbonaceous aerosol pollution was driven to a large (often dominant) extent by SOA formation from both, fossil and biomass-burning sources (Zhang et al., 2015b). For all four cities, the 24 h average levels of WSOC were significantly correlated with the levels of $PM_{2.5}$ and OC (R=0.99, p<0.01, Figure 2), suggesting that WSOC and OA may have similar sources and formation processes and thus have important implications for OC loadings and associated environmental and health effects. However, the sources of WSOC remain poorly constrained. In this study, we measured the ^{14}C content of WSOC aerosols in six samples (three with the highest, three with average PM mass) for each city to report on heavily and moderately polluted days (HPD and MPD, respectively) (Zhang et al., 2015b). The ^{14}C contents of OC and EC of the same samples were reported previously (Zhang et al., 2015b).

WSOC on average accounted for 53±8.0% (ranging from 40-65%) of OC including all samples from the four sites, which was consistent with previous estimates . Based on these measurements, the concentrations of WSOC from non-fossil sources ($WSOC_{NF}$) spanned from 1.41 to 45.3 μg/m^3 with a mean of 10.6±12.1 μg/m^3, whereas the corresponding range for WSOC from fossil-fuel emissions ($WSOC_F$) was 0.44 to 20.1 μg/m^3 with a mean of 5.3±4.9 μg/m^3 (Figure 3). Similar to $PM_{2.5}$ levels, the highest concentrations of $WSOC_{NF}$ and $WSOC_F$ were observed in Northern China in Xi'an and Beijing (Xi'an>Beijing), followed by the two southern sites Shanghai and Guangzhou. Non-fossil contributions (mean ± standard deviation)

to total WSOC were 53±5%, 75±4%, 48±2% and 68±6% in Beijing, Xi'an, Shanghai, and Guangzhou, respectively. Thus, fossil contributions were notably higher in Beijing and Shanghai than those in Xi'an and Guangzhou. Such a trend was also observed for OC (Zhang et al., 2015b), suggesting relatively high contribution from fossil-fuel emissions to OC and WSOC due to large coal usage. Despite of these fossil emissions, non-fossil sources were considerably important or even dominant contributors for all the studied sites, which may be associated with primary and secondary OA from regional-transported and local biomass burning emissions. As shown in Figure 4, non-fossil WSOC was significantly correlated with levoglucosan, indicating that a large fraction of non-fossil WSOC was indeed from biomass burning emissions. In addition, no significant or only a negative correlation (Figure 4) was found between levoglucosan and fraction of fossil to WSOC, suggesting that fossil-fuel source is very unlikely a major or important contributor of levoglucosan even in the regions (e.g., Xi'an and Beijing in this study) where coal combustion is important during the cold period (Zhang et al., 2015a). It should also be noted that formation of SOA derived from biogenic VOCs may also have contributed to $WSOC_{NF}$ in Guangzhou, where temperatures during the sampling period were significantly higher (i.e., 5–18 °C) than those in other cities (i.e., -12 to +9 °C)(Bozzetti et al., 2017b). Although both fossil and non-fossil WSOC concentrations were dramatically enhanced during HPD compared to those during MPD, their relative contributions did not change significantly in Beijing and Shanghai whereas a small increasing and decreasing trend in non-fossil fraction was found in Xi'an and Guangzhou, respectively (Figure 3). This suggests that the source pattern of WSOC in Beijing and Shanghai remained similar between HPD and MPD, but the increase in the WSOC concentrations was rather enhanced by additional fossil-fuel and biogenic/biomass burning emissions in Guangzhou and Xi'an, respectively. It should be noted that the meteorological conditions play significant roles on the haze formation in the eastern China during winter 2013, and has already been well documented (Zhang et al., 2014a). However, the details sources of WSOC and WIOC were still unclear.

3.2 WSOC versus WIOC

To compare sources of WSOC and WIOC aerosols, the mass concentrations and ^{14}C contents of WIOC were also derived based on mass balance. The ^{14}C-based source apportionment of WIOC and the relationship between f_{NF}(WSOC) and f_{NF}(WIOC) is presented in Figures 5 and 6a, respectively. It shows that non-fossil contributions to WSOC were larger than those of WIOC for nearly all samples in Beijing, Xi'an and Guangzhou. On average, the majority (60-70%) of the fossil OC was water insoluble at these 3 sites (see Figure 6b), indicating that fossil-derived OA mostly consisted of hydrophobic components and thus is less water soluble than OA from non-fossil sources. This result is consistent with findings reported elsewhere such as at an urban or rural site in Switzerland (Zhang et al., 2013), a remote site in Hainan Island, South China (Zhang et al., 2014b) and at two rural sites on the east coast of the United States (Wozniak et al., 2012). Meanwhile, the fossil OC in Shanghai, the dominant fraction of OC, was more water soluble (Figure 6b), suggesting an enhanced SOA formation from fossil VOCs from vehicle emissions and/or coal burning for this city. As shown in Figure 6b, non-fossil OA was enriched in water-soluble fractions (i.e., 60%±8%) for all cities, associated with the hydrophilic properties of biogenic-derived SOA and biomass-burning derived primary organic aerosol (POA) and SOA, which are composed of a large fraction of polar and highly oxygenated compounds (Mayol-Bracero et al., 2002;Sullivan et al., 2011;Noziere et al., 2015). Thus, non-fossil OC has more water-soluble components than fossil ones. It should be noted that relative contributions of $WSOC_{NF}$ and $WSOC_{F}$ are similar in Beijing and Shanghai, whereas $WSOC_{NF}$ is much higher than $WSOC_{F}$ in Xi'an and Guangzhou. This suggests larger contribution of non-fossil sources to WSOC aerosols in Xi'an and Guangzhou than those in Beijing and Shanghai.

3.3 High contribution of secondary formation to WSOC

WSOC was further apportioned into fossil sources such as coal burning (CB), traffic (TR) and SOC (SOC,F) as well as non-fossil sources such as biomass burning (BB), cooking (CI) and SOC (SOC,NF) using a AMS[2] based source apportionment (see Sec. 2.5 and Figure 1). SOC dominated WSOC during both the HPD and MPD with a mean contribution of 67%±9%, highlighting the importance of SOC formation to the WSOC aerosols in wintertime pollution

events. This is consistent with our previous findings for total $PM_{2.5}$ mass and bulk carbonaceous aerosols (i.e., total carbon, sum of OC and EC) (Huang et al., 2014;Zhang et al., 2015b). The increase in SOC contribution to WSOC during HPD compared to MPD can be largely due to fossil contribution in Beijing but non-fossil emissions in Xi'an. In Shanghai and Guangzhou, the source pattern of WSOC was not significantly different between MPD and HPD. Fossil contributions to $WSOC_{SOC}$ were 50%±9% in Beijing, 61±4% in Shanghai, associated with SOA from local and transported fossil-fuel derived precursors at these sites (Guo et al., 2014). This contribution drops to 36±9% and 26±9% in Guangzhou and Xi'an, respectively, due to higher biomass-burning contribution to SOC. Despite of the general importance of fossil SOC, formation of non-fossil $WSOC_{SOC}$ becomes especially relevant during HPD especially in Xi'an (Figure 7), which may be explained by competing effects in SOC formation from fossil versus non-fossil precursors. It can be hypothesized for extremely polluted episodes that more hydrophilic volatile compounds that were emitted from biomass burning precursors preferentially form SOC compounds via heterogeneous reaction/processing on dust particles compared to highly hydrophobic precursors from fossil sources, a point subjected to future laboratory and field experiments. The most important primary sources of WSOC were biomass burning emissions, and their contributions were higher in Xi'an (26%±7%) and Guangzhou (25%±6%) than those found in Beijing (17%±6%) and Shanghai (17%±5%). The remaining primary sources such as coal combustion, cooking and traffic were generally very small contributors of WSOC due to lower water solubility, although coal combustion could exceed 10% in Beijing. It should be noted that WSOC was dominated by SOC formation with mean contribution of 61%±10% and 72%±12% (average for all four cities) to non-fossil and fossil-fuel derived WSOC, respectively.

Summary and implications

Our study demonstrates that non-fossil emissions are generally a dominant contributor of WSOC aerosols during extreme haze events in representative major cities of China, which is in agreement with WSOC source information identified in aerosols with different size fractions

(e.g., TSP, PM_{10} and $PM_{2.5}$) observed in the Northern Hemisphere at urban, rural, semi-urban, and background sites in East/South Asia, Europe and USA (Table 1). The ^{14}C-based source apportionment database shows a mean non-fossil fraction of 73±11% across all sites. This overwhelming non-fossil contribution to WSOC is consistently observed throughout the year, which is associated with seasonal-dependent biomass-burning emissions and/or biogenic-derived SOC formation. Our study provides evidence that the presence of oxidized OA, which is to a large extent water soluble, in the Northern Hemisphere (Zhang et al., 2007) is mainly derived from biogenic-derived SOA and/or biomass burning sources. The overall importance of non-fossil emissions to the WSOC aerosols results from large contributions of SOC formation from biogenic precursors (e.g., most likely during summer) and relatively high water-solubility of primary biomass burning particles (e.g., most likely during winter) compared to those emitted from fossil fuel emissions such as coal combustion and vehicle exhaust. Despite of the importance of non-fossil sources, a significant fossil fraction is also observed in the WSOC aerosols from polluted regions in East Asia and sites influenced by East Asian continental outflow (Table 1, Figure 8). This fossil contribution is apparently higher than in this region than in the USA and Europe, which is due to large industrial and residential coal usage as well as vehicle emissions. From our observation, the increases in the fossil fractions of WSOC were mostly from SOC formation. Since WSOC has hygroscopic properties, our findings suggest that SOC formation from non-fossil emissions have significant implications on aerosol-induced climate effects. In addition, fossil-derived SOC formation may also become important in polluted regions with large amounts of fossil fuel emissions such as in China and other emerging countries. Low combustion efficiencies and consequently high emission factors in most of the combustion processes in China may further be responsible for increased concentrations of fossil precursors which may be oxidized to form water-soluble SOA in the atmosphere and contribute substantially to the WSOC aerosols. The enhanced WSOC levels may be also originate from aging of fossil POA during the long-range transport of aerosols (Kirillova et al., 2014a). It is also interesting to note that fossil contribution during winter in East Asia is generally higher than those in the rest of the year although relatively large fossil

fraction could be occasionally found as well. Such seasonal dependence was not observed in other regions, suggesting the importance of fossil contribution to WSOC due to increasing coal combustions during winter in China. This study provides a more detailed source apportionment of WSOC, which could improve modelling of climate and health effects as well as the understanding of atmospheric chemistry of WSOC in the polluted atmosphere such as China and provide scientific basis for policy decisions on air pollution emissions mitigation.

REFERENCES

Andreae, M. O., and Gelencser, A.: Black carbon or brown carbon? The nature of light-absorbing carbonaceous aerosols, Atmos. Chem. Phys., 6, 3131-3148, 2006.

Asa-Awuku, A., Moore, R. H., Nenes, A., Bahreini, R., Holloway, J. S., Brock, C. A., Middlebrook, A. M., Ryerson, T. B., Jimenez, J. L., DeCarlo, P. F., Hecobian, A., Weber, R. J., Stickel, R., Tanner, D. J., and Huey, L. G.: Airborne cloud condensation nuclei measurements during the 2006 Texas Air Quality Study, J. Geophys. Res., 116, D11201, doi:10.1029/2010jd014874, 2011.

Bosch, C., Andersson, A., Kirillova, E. N., Budhavant, K., Tiwari, S., Praveen, P. S., Russell, L. M., Beres, N. D., Ramanathan, V., and Gustafsson, O.: Source-diagnostic dual-isotope composition and optical properties of water-soluble organic carbon and elemental carbon in the South Asian outflow intercepted over the Indian Ocean, J. Geophys. Res., 119, 11743-11759, doi:10.1002/2014JD022127, 2014.

Bozzetti, C., El Haddad, I., Salameh, D., Daellenbach, K. R., Fermo, P., Gonzalez, R., Minguillón, M. C., Iinuma, Y., Poulain, L., Elser, M., Müller, E., Slowik, J. G., Jaffrezo, J. L., Baltensperger, U., Marchand, N., and Prévôt, A. S. H.: Organic aerosol source apportionment by offline-AMS over a full year in Marseille, Atmos. Chem. Phys., 17, 8247-8268, doi:10.5194/acp-17-8247-2017, 2017a.

Bozzetti, C., Sosedova, Y., Xiao, M., Daellenbach, K. R., Ulevicius, V., Dudoitis, V., Mordas, G., Byčenkienė, S., Plauškaitė, K., Vlachou, A., Golly, B., Chazeau, B., Besombes, J. L., Baltensperger, U., Jaffrezo, J. L., Slowik, J. G., El Haddad, I., and Prévôt, A. S. H.: Argon

401 offline-AMS source apportionment of organic aerosol over yearly cycles for an urban, rural,
402 and marine site in northern Europe, Atmos. Chem. Phys., 17, 117-141, doi:10.5194/acp-17-
403 117-2017, 2017b.
404 Canonaco, F., Crippa, M., Slowik, J. G., Baltensperger, U., and Prévôt, A. S. H.: SoFi, an
405 IGOR-based interface for the efficient use of the generalized multilinear engine (ME-2) for the
406 source apportionment: ME-2 application to aerosol mass spectrometer data, Atmos. Meas.
407 Tech., 6, 3649-3661, doi:10.5194/amt-6-3649-2013, 2013.
408 Cao, F., Zhang, Y.-L., Szidat, S., Zapf, A., Wacker, L., and Schwikowski, M.: Microgram-level
409 radiocarbon determination of carbonaceous particles in firn and ice samples: pretreatment and
410 OC/EC separation, Radiocarbon, 55, 383-390, 2013.
411 Cao, F., Zhang, Y., Ren, L., Liu, J., Li, J., Zhang, G., Liu, D., Sun, Y., Wang, Z., Shi, Z., and
412 Fu, P.: New insights into the sources and formation of carbonaceous aerosols in China: potential
413 applications of dual-carbon isotopes, National Science Review, nwx097-nwx097,
414 doi:10.1093/nsr/nwx097, 2017.
415 Cavalli, F., Viana, M., Yttri, K. E., Genberg, J., and Putaud, J. P.: Toward a standardised
416 thermal-optical protocol for measuring atmospheric organic and elemental carbon: the
417 EUSAAR protocol, Atmos. Meas. Tech., 3, 79-89, 2010.
418 Cheng, Y., He, K. B., Zheng, M., Duan, F. K., Du, Z. Y., Ma, Y. L., Tan, J. H., Yang, F. M.,
419 Liu, J. M., Zhang, X. L., Weber, R. J., Bergin, M. H., and Russell, A. G.: Mass absorption
420 efficiency of elemental carbon and water-soluble organic carbon in Beijing, China, Atmos.
421 Chem. Phys., 11, 11497-11510, doi:10.5194/acp-11-11497-2011, 2011.
422 Daellenbach, K. R., Bozzetti, C., Krepelova, A. K., Canonaco, F., Wolf, R., Zotter, P., Fermo,
423 P., Crippa, M., Slowik, J. G., Sosedova, Y., Zhang, Y., Huang, R. J., Poulain, L., Szidat, S.,
424 Baltensperger, U., El Haddad, I., and Prevot, A. S. H.: Characterization and source
425 apportionment of organic aerosol using offline aerosol mass spectrometry, Atmos. Meas. Tech.,
426 9, 23-39, doi:10.5194/amt-9-23-2016, 2016.
427 Dusek, U., Hitzenberger, R., Kasper-Giebl, A., Kistler, M., Meijer, H. A. J., Szidat, S., Wacker,
428 L., Holzinger, R., and Röckmann, T.: Sources and formation mechanisms of carbonaceous

aerosol at a regional background site in the Netherlands: insights from a year-long radiocarbon study, Atmos. Chem. Phys., 17, 3233-3251, doi:10.5194/acp-17-3233-2017, 2017.

Fang, W., Andersson, A., Zheng, M., Lee, M., Holmstrand, H., Kim, S.-W., Du, K., and Gustafsson, Ö.: Divergent Evolution of Carbonaceous Aerosols during Dispersal of East Asian Haze, Scientific Reports, 7, 10422, doi:10.1038/s41598-017-10766-4, 2017.

Fu, P., Kawamura, K., Chen, J., Qin, M., Ren, L., Sun, Y., Wang, Z., Barrie, L. A., Tachibana, E., Ding, A., and Yamashita, Y.: Fluorescent water-soluble organic aerosols in the High Arctic atmosphere, Sci Rep, 5, 9845, doi:10.1038/srep09845, 2015.

Guo, S., Hu, M., Zamora, M. L., Peng, J., Shang, D., Zheng, J., Du, Z., Wu, Z., Shao, M., Zeng, L., Molina, M. J., and Zhang, R.: Elucidating severe urban haze formation in China, Proc. Nat. Acad. Sci. U.S.A., 111, 17373-17378, doi:10.1073/pnas.1419604111, 2014.

Hecobian, A., Zhang, X., Zheng, M., Frank, N., Edgerton, E. S., and Weber, R. J.: Water-Soluble Organic Aerosol material and the light-absorption characteristics of aqueous extracts measured over the Southeastern United States, Atmos. Chem. Phys., 10, 5965-5977, doi:10.5194/acp-10-5965-2010, 2010.

Huang, R. J., Zhang, Y., Bozzetti, C., Ho, K. F., Cao, J. J., Han, Y., Daellenbach, K. R., Slowik, J. G., Platt, S. M., Canonaco, F., Zotter, P., Wolf, R., Pieber, S. M., Bruns, E. A., Crippa, M., Ciarelli, G., Piazzalunga, A., Schwikowski, M., Abbaszade, G., Schnelle-Kreis, J., Zimmermann, R., An, Z., Szidat, S., Baltensperger, U., El Haddad, I., and Prevot, A. S.: High secondary aerosol contribution to particulate pollution during haze events in China, Nature, 514, 218-222, doi:10.1038/nature13774, 2014.

Jimenez, J. L., Canagaratna, M. R., Donahue, N. M., Prevot, A. S. H., Zhang, Q., Kroll, J. H., DeCarlo, P. F., Allan, J. D., Coe, H., Ng, N. L., Aiken, A. C., Docherty, K. S., Ulbrich, I. M., Grieshop, A. P., Robinson, A. L., Duplissy, J., Smith, J. D., Wilson, K. R., Lanz, V. A., Hueglin, C., Sun, Y. L., Tian, J., Laaksonen, A., Raatikainen, T., Rautiainen, J., Vaattovaara, P., Ehn, M., Kulmala, M., Tomlinson, J. M., Collins, D. R., Cubison, M. J., Dunlea, E. J., Huffman, J. A., Onasch, T. B., Alfarra, M. R., Williams, P. I., Bower, K., Kondo, Y., Schneider, J., Drewnick, F., Borrmann, S., Weimer, S., Demerjian, K., Salcedo, D., Cottrell, L., Griffin, R.,

Takami, A., Miyoshi, T., Hatakeyama, S., Shimono, A., Sun, J. Y., Zhang, Y. M., Dzepina, K., Kimmel, J. R., Sueper, D., Jayne, J. T., Herndon, S. C., Trimborn, A. M., Williams, L. R., Wood, E. C., Middlebrook, A. M., Kolb, C. E., Baltensperger, U., and Worsnop, D. R.: Evolution of organic aerosols in the atmosphere, Science, 326, 1525-1529, doi:DOI 10.1126/science.1180353, 2009.

Kirillova, E. N., Sheesley, R. J., Andersson, A., and Gustafsson, O.: Natural abundance ^{13}C and ^{14}C analysis of water-soluble organic carbon in atmospheric aerosols, Anal. Chem., 82, 7973-7978, doi:Doi 10.1021/Ac1014436, 2010.

Kirillova, E. N., Andersson, A., Sheesley, R. J., Kruså, M., Praveen, P. S., Budhavant, K., Safai, P. D., Rao, P. S. P., and Gustafsson, Ö.: ^{13}C and ^{14}C-based study of sources and atmospheric processing of water-soluble organic carbon (WSOC) in South Asian aerosols, J. Geophys. Res., 118, 614-626, doi:10.1002/jgrd.50130, 2013.

Kirillova, E. N., Andersson, A., Han, J., Lee, M., and Gustafsson, O.: Sources and light absorption of water-soluble organic carbon aerosols in the outflow from northern China, Atmos. Chem. Phys., 14, 1413-1422, doi:DOI 10.5194/acp-14-1413-2014, 2014a.

Kirillova, E. N., Andersson, A., Tiwari, S., Srivastava, A. K., Bisht, D. S., and Gustafsson, O.: Water-soluble organic carbon aerosols during a full New Delhi winter: Isotope-based source apportionment and optical properties, J. Geophys. Res., 119, 3476-3485, doi:Doi 10.1002/2013jd020041, 2014b.

Kondo, Y., Miyazaki, Y., Takegawa, N., Miyakawa, T., Weber, R. J., Jimenez, J. L., Zhang, Q., and Worsnop, D. R.: Oxygenated and water-soluble organic aerosols in Tokyo, J. Geophys. Res., 112, D01203, doi:10.1029/2006jd007056, 2007.

Laskin, A., Laskin, J., and Nizkorodov, S. A.: Chemistry of Atmospheric Brown Carbon, Chem. Rev. (Washington, DC, U. S.), 115, 4335-4382, doi:10.1021/cr5006167, 2015.

Levin, I., Naegler, T., Kromer, B., Diehl, M., Francey, R. J., Gomez-Pelaez, A. J., Steele, L. P., Wagenbach, D., Weller, R., and Worthy, D. E.: Observations and modelling of the global distribution and long-term trend of atmospheric $^{14}CO_2$, Tellus B, 62, 26-46, doi:10.1111/j.1600-0889.2009.00446.x, 2010.

Limbeck, A., Handler, M., Neuberger, B., Klatzer, B., and Puxbaum, H.: Carbon-specific analysis of humic-like substances in atmospheric aerosol and precipitation samples, Anal. Chem., 77, 7288-7293, doi:10.1021/ac050953l, 2005.

Liu, J., Li, J., Vonwiller, M., Liu, D., Cheng, H., Shen, K., Salazar, G., Agrios, K., Zhang, Y., He, Q., Ding, X., Zhong, G., Wang, X., Szidat, S., and Zhang, G.: The importance of non-fossil sources in carbonaceous aerosols in a megacity of central China during the 2013 winter haze episode: A source apportionment constrained by radiocarbon and organic tracers, Atmos. Environ., 144, 60-68, doi:http://dx.doi.org/10.1016/j.atmosenv.2016.08.068, 2016.

Liu, J. W., Li, J., Zhang, Y. L., Liu, D., Ding, P., Shen, C. D., Shen, K. J., He, Q. F., Ding, X., Wang, X. M., Chen, D. H., Szidat, S., and Zhang, G.: Source Apportionment Using Radiocarbon and Organic Tracers for PM2.5 Carbonaceous Aerosols in Guangzhou, South China: Contrasting Local- and Regional-Scale Haze Events, Environ. Sci. Technol., 48, 12002-12011, doi:Doi 10.1021/Es503102w, 2014.

Mayol-Bracero, O. L., Guyon, P., Graham, B., Roberts, G., Andreae, M. O., Decesari, S., Facchini, M. C., Fuzzi, S., and Artaxo, P.: Water-soluble organic compounds in biomass burning aerosols over Amazonia - 2. Apportionment of the chemical composition and importance of the polyacidic fraction, J. Geophys. Res., 107, D8091, doi:10.1029/2001jd000522, 2002.

Miyazaki, Y., Kondo, Y., Takegawa, N., Komazaki, Y., Fukuda, M., Kawamura, K., Mochida, M., Okuzawa, K., and Weber, R. J.: Time-resolved measurements of water-soluble organic carbon in Tokyo, J. Geophys. Res., 111, D23206, doi:1029/2006jd007125, 2006.

Mohn, J., Szidat, S., Fellner, J., Rechberger, H., Quartier, R., Buchmann, B., and Emmenegger, L.: Determination of biogenic and fossil CO_2 emitted by waste incineration based on $^{14}CO_2$ and mass balances, Bioresour. Technol., 99, 6471-6479, doi:DOI 10.1016/j.biortech.2007.11.042, 2008.

Noziere, B., Kalberer, M., Claeys, M., Allan, J., D'Anna, B., Decesari, S., Finessi, E., Glasius, M., Grgic, I., Hamilton, J. F., Hoffmann, T., Iinuma, Y., Jaoui, M., Kahnt, A., Kampf, C. J., Kourtchev, I., Maenhaut, W., Marsden, N., Saarikoski, S., Schnelle-Kreis, J., Surratt, J. D.,

513 Szidat, S., Szmigielski, R., and Wisthaler, A.: The molecular identification of organic
514 compounds in the atmosphere: state of the art and challenges, Chem Rev, 115, 3919-3983,
515 doi:10.1021/cr5003485, 2015.
516 Pavuluri, C. M., Kawamura, K., Uchida, M., Kondo, M., and Fu, P. Q.: Enhanced modern
517 carbon and biogenic organic tracers in Northeast Asian aerosols during spring/summer, J.
518 Geophys. Res., 118, 2362-2371, doi:Doi 10.1002/Jgrd.50244, 2013.
519 Ruellan, S., and Cachier, H.: Characterisation of fresh particulate vehicular exhausts near a
520 Paris high flow road, Atmos. Environ., 35, 453-468, doi:Doi 10.1016/S1352-2310(00)00110-
521 2, 2001.
522 Salazar, G., Zhang, Y. L., Agrios, K., and Szidat, S.: Development of a method for fast and
523 automatic radiocarbon measurement of aerosol samples by online coupling of an elemental
524 analyzer with a MICADAS AMS, Nucl. Instr. and Meth. in Phys. Res. B., 361, 163-167,
525 doi:http://dx.doi.org/10.1016/j.nimb.2015.03.051, 2015.
526 Sannigrahi, P., Sullivan, A. P., Weber, R. J., and Ingall, E. D.: Characterization of water-soluble
527 organic carbon in urban atmospheric aerosols using solid-state C-13 NMR spectroscopy,
528 Environ. Sci. Technol., 40, 666-672, doi:Doi 10.1021/Es051150i, 2006.
529 Stuiver, M.: Discussion: Reporting of ^{14}C data, Radiocarbon, 19, 355-363, 1977.
530 Sullivan, A. P., Frank, N., Kenski, D. M., and Collett, J. L.: Application of high-performance
531 anion-exchange chromatography-pulsed amperometric detection for measuring carbohydrates
532 in routine daily filter samples collected by a national network: 2. Examination of sugar
533 alcohols/polyols, sugars, and anhydrosugars in the upper Midwest, J. Geophys. Res., 116,
534 D08303, doi:10.1029/2010jd014169, 2011.
535 Szidat, S., Jenk, T. M., Gäggeler, H. W., Synal, H. A., Fisseha, R., Baltensperger, U., Kalberer,
536 M., Samburova, V., Wacker, L., Saurer, M., Schwikowski, M., and Hajdas, I.: Source
537 apportionment of aerosols by ^{14}C measurements in different carbonaceous particle fractions,
538 Radiocarbon, 46, 475-484, 2004.

Szidat, S., Ruff, M., Perron, N., Wacker, L., Synal, H.-A., Hallquist, M., Shannigrahi, A. S., Yttri, K. E., Dye, C., and Simpson, D.: Fossil and non-fossil sources of organic carbon (OC) and elemental carbon (EC) in Goeteborg, Sweden, Atmos. Chem. Phys., 9, 1521-1535, 2009.

Timonen, H., Carbone, S., Aurela, M., Saarnio, K., Saarikoski, S., Ng, N. L., Canagaratna, M. R., Kulmala, M., Kerminen, V. M., Worsnop, D. R., and Hillamo, R.: Characteristics, sources and water-solubility of ambient submicron organic aerosol in springtime in Helsinki, Finland, J. Aerosol Sci., 56, 61-77, doi:10.1016/j.jaerosci.2012.06.005, 2013.

Wacker, L., Fahrni, S. M., Hajdas, I., Molnar, M., Synal, H. A., Szidat, S., and Zhang, Y. L.: A versatile gas interface for routine radiocarbon analysis with a gas ion source, Nucl. Instrum. Meth. B, 294, 315-319, doi:DOI 10.1016/j.nimb.2012.02.009, 2013.

Weber, R. J., Sullivan, A. P., Peltier, R. E., Russell, A., Yan, B., Zheng, M., de Gouw, J., Warneke, C., Brock, C., Holloway, J. S., Atlas, E. L., and Edgerton, E.: A study of secondary organic aerosol formation in the anthropogenic-influenced southeastern United States, J. Geophys. Res., 112, D13302, doi:10.1029/2007jd008408, 2007.

Wozniak, A. S., Bauer, J. E., and Dickhut, R. M.: Characteristics of water-soluble organic carbon associated with aerosol particles in the eastern United States, Atmos. Environ., 46, 181-188, doi:DOI 10.1016/j.atmosenv.2011.10.001, 2012.

Xiao, R., Takegawa, N., Zheng, M., Kondo, Y., Miyazaki, Y., Miyakawa, T., Hu, M., Shao, M., Zeng, L., Gong, Y., Lu, K., Deng, Z., Zhao, Y., and Zhang, Y. H.: Characterization and source apportionment of submicron aerosol with aerosol mass spectrometer during the PRIDE-PRD 2006 campaign, Atmos. Chem. Phys., 11, 6911-6929, doi:10.5194/acp-11-6911-2011, 2011.

Yan, C., Zheng, M., Bosch, C., Andersson, A., Desyaterik, Y., Sullivan, A. P., Collett, J. L., Zhao, B., Wang, S., He, K., and Gustafsson, O.: Important fossil source contribution to brown carbon in Beijing during winter, Sci Rep, 7, 43182, doi:10.1038/srep43182, 2017.

Zappoli, S., Andracchio, A., Fuzzi, S., Facchini, M. C., Gelencser, A., Kiss, G., Krivacsy, Z., Molnar, A., Meszaros, E., Hansson, H. C., Rosman, K., and Zebuhr, Y.: Inorganic, organic and macromolecular components of fine aerosol in different areas of Europe in relation to their

566 water solubility, Atmos. Environ., 33, 2733-2743, doi:Doi 10.1016/S1352-2310(98)00362-8,
567 1999.
568 Zhang, Q., Jimenez, J. L., Canagaratna, M. R., Allan, J. D., Coe, H., Ulbrich, I., Alfarra, M. R.,
569 Takami, A., Middlebrook, A. M., Sun, Y. L., Dzepina, K., Dunlea, E., Docherty, K., DeCarlo,
570 P. F., Salcedo, D., Onasch, T., Jayne, J. T., Miyoshi, T., Shimono, A., Hatakeyama, S.,
571 Takegawa, N., Kondo, Y., Schneider, J., Drewnick, F., Borrmann, S., Weimer, S., Demerjian,
572 K., Williams, P., Bower, K., Bahreini, R., Cottrell, L., Griffin, R. J., Rautiainen, J., Sun, J. Y.,
573 Zhang, Y. M., and Worsnop, D. R.: Ubiquity and dominance of oxygenated species in organic
574 aerosols in anthropogenically-influenced Northern Hemisphere midlatitudes, Geophys. Res.
575 Lett., 34, L13801, doi:DOI:10.1029/2007gl029979, 2007.
576 Zhang, R., Li, Q., and Zhang, R.: Meteorological conditions for the persistent severe fog and
577 haze event over eastern China in January 2013, SCIENCE CHINA Earth Sciences, 57, 26-35,
578 doi:10.1007/s11430-013-4774-3, 2014a.
579 Zhang, Y.-L., Li, J., Zhang, G., Zotter, P., Huang, R.-J., Tang, J.-H., Wacker, L., Prévôt, A. S.
580 H., and Szidat, S.: Radiocarbon-based source apportionment of carbonaceous aerosols at a
581 regional background site on hainan Island, South China, Environ. Sci. Technol., 48, 2651-2659,
582 doi:10.1021/es4050852, 2014b.
583 Zhang, Y.-L., Liu, J.-W., Salazar, G. A., Li, J., Zotter, P., Zhang, G., Shen, R.-r., Schäfer, K.,
584 Schnelle-Kreis, J., Prévôt, A. S. H., and Szidat, S.: Micro-scale (μg) radiocarbon analysis of
585 water-soluble organic carbon in aerosol samples, Atmos. Environ., 97, 1-5,
586 doi:http://dx.doi.org/10.1016/j.atmosenv.2014.07.059, 2014c.
587 Zhang, Y.-L., Schnelle-Kreis, J. r., Abbaszade, G. l., Zimmermann, R., Zotter, P., Shen, R.-r.,
588 Schäfer, K., Shao, L., Prévôt, A. S. H., and Szidat, S. n.: Source apportionment of elemental
589 carbon in Beijing, China: Insights from radiocarbon and organic marker measurements,
590 Environ. Sci. Technol., 49, 8408-8415, 2015a.
591 Zhang, Y., Ren, H., Sun, Y., Cao, F., Chang, Y., Liu, S., Lee, X., Agrios, K., Kawamura, K.,
592 Liu, D., Ren, L., Du, W., Wang, Z., Prevot, A. S. H., Szidat, S., and Fu, P.: High Contribution

of Nonfossil Sources to Submicrometer Organic Aerosols in Beijing, China, Environ. Sci. Technol., 51, 7842-7852, doi:10.1021/acs.est.7b01517, 2017.

Zhang, Y. L., Perron, N., Ciobanu, V. G., Zotter, P., Minguillón, M. C., Wacker, L., Prévôt, A. S. H., Baltensperger, U., and Szidat, S.: On the isolation of OC and EC and the optimal strategy of radiocarbon-based source apportionment of carbonaceous aerosols, Atmos. Chem. Phys., 12, 10841-10856, 2012.

Zhang, Y. L., Zotter, P., Perron, N., Prévôt, A. S. H., Wacker, L., and Szidat, S.: Fossil and non-fossil sources of different carbonaceous fractions in fine and coarse particles by radiocarbon measurement, Radiocarbon, 55, 1510-1520, 2013.

Zhang, Y. L., Huang, R. J., El Haddad, I., Ho, K. F., Cao, J. J., Han, Y., Zotter, P., Bozzetti, C., Daellenbach, K. R., Canonaco, F., Slowik, J. G., Salazar, G., Schwikowski, M., Schnelle-Kreis, J., Abbaszade, G., Zimmermann, R., Baltensperger, U., Prévôt, A. S. H., and Szidat, S.: Fossil vs. non-fossil sources of fine carbonaceous aerosols in four Chinese cities during the extreme winter haze episode of 2013, Atmos. Chem. Phys., 15, 1299-1312, doi:10.5194/acp-15-1299-2015, 2015b.

Zong, Z., Wang, X., Tian, C., Chen, Y., Han, G., Li, J., and Zhang, G.: Source and formation characteristics of water-soluble organic carbon in the anthropogenic-influenced Yellow River Delta, North China, Atmos. Environ., 144, 124-132, doi:https://doi.org/10.1016/j.atmosenv.2016.08.078, 2016.

Zotter, P., Ciobanu, V. G., Zhang, Y. L., El-Haddad, I., Macchia, M., Daellenbach, K. R., Salazar, G. A., Huang, R. J., Wacker, L., Hueglin, C., Piazzalunga, A., Fermo, P., Schwikowski, M., Baltensperger, U., Szidat, S., and Prévôt, A. S. H.: Radiocarbon analysis of elemental and organic carbon in Switzerland during winter-smog episodes from 2008 to 2012 – Part 1: Source apportionment and spatial variability, Atmos. Chem. Phys., 14, 13551-13570, doi:10.5194/acp-14-13551-2014, 2014a.

Zotter, P., El-Haddad, I., Zhang, Y., Hayes, P. L., Zhang, X., Lin, Y.-H., Wacker, L., Schnelle-Kreis, J., Abbaszade, G., Zimmermann, R., Surratt, J. D., Weber, R., Jimenez, J. L., Szidat, S., Baltensperger, U., and Prévôt, A. S. H.: Diurnal cycle of fossil and nonfossil carbon using

radiocarbon analyses during CalNex, J. Geophys. Res., 119, 6818-6835, doi:10.1002/2013jd021114, 2014b.

Author Contributions: Y.-L.Z., S.S., R.J.H., J.J.C. and A.S.H.P. designed the study. Y.L.Z. and G.S. perform ^{14}C measurement. Y.L.Z. and S. S. interpreted the ^{14}C data. R.J.H., I.E.H., C.B. and K.D. performed the offline AMS analysis and interpret the data. Y.-L.Z. and I.E.H. perform ^{14}C-AMS-PMF source apportionments. Y.-L.Z. wrote the paper. All authors reviewed and commented on the paper.

Competing interests: The authors declare no competing financial interests.

Acknowledgments: This work was supported by The National Key Research and Development Program of China (Grant No. SQ2017ZY010322-04), the National Natural Science Foundation of China (Grant Nos. 41603104 and 91644103) and the Priority Academic Program Development of Jiangsu Higher Education Institutions (grant PAOD). All data needed to evaluate the conclusions in the paper are present in the paper. Additional data related to this paper may be requested from the authors.

Figures and Tables

Table 1. Compilation of literature values of relative fossil-fuel contributions (fossil %) to the WSOC aerosols in East/South Asia, USA and Europe.

Site	Location	Season	Size	WSOC ($\mu g/m^3$)	WSOC/OC	Fossil %	References
East Asia							
Urban	Beijing, China	Winter/2013	$PM_{2.5}$	19.8	0.49	47	this work
Urban	Xi'an, China	Winter/2013	$PM_{2.5}$	31.3	0.53	25	this work
Urban	Shanghai, China	Winter/2013	$PM_{2.5}$	6.5	0.58	52	this work
Urban	Guangzhou, China	Winter/2013	$PM_{2.5}$	6.6	0.53	32	this work
Urban	Beijing, China	Winter/2014	$PM_{2.5}$	14.7	0.40	56	(Fang et al., 2017)
Urban	Beijing, China	Winter/2011	$PM_{4.3}$	15	0.50	55	(Zhang et al., 2014c)
Urban	Beijing, China	Winter/2013	$PM_{2.5}$	9.3	0.31	54	(Yan et al., 2017)
Urban	Guangzhou, China	Winter/2012/ 2013	$PM_{2.5}$	4.1	0.38	33	(Liu et al., 2014)
Urban	Guangzhou, China	Winter/2011	PM_{10}	4.5	0.43	28.5	(Zhang et al., 2014c)
Urban	Xi'an, China	Autumn/2009	$PM_{2.5}$	5.1	0.28	31	(Pavuluri et al., 2013)
Urban	Xi'an, China	Autumn/2010	TSP	8.1	0.28	29	(Pavuluri et al., 2013)
Urban	Wuhan, China	Winter/2013	$PM_{2.5}$	13.7	0.45	37	(Liu et al., 2016)
Urban	Sapporo, Japan	Summer/Autum n/2010	PM_3	1	0.43	15	(Pavuluri et al., 2013)
Urban	Sapporo, Japan	Summer/2011	TSP	1.1	0.24	12	(Pavuluri et al., 2013)
Urban	Sapporo, Japan	Spring/2010	TSP	1.1	0.31	11	(Pavuluri et al., 2013)
Urban	Sapporo, Japan	Autumn/2011	TSP	1.8	0.48	18.3	(Pavuluri et al., 2013)
Urban	Sapporo, Japan	Winter/2010	TSP	0.9	0.45	40.2	(Pavuluri et al., 2013)
Background	Jeju Island, Korea	Winter/2014	$PM_{2.5}$	2.2	0.66	50	*(Fang et al., 2017)*
Background	Jeju Island, Korea	Spring/2011	$PM_{2.5}$	2.0		37.5	*(Kirillova et al., 2014a)*
Background	Jeju Island, Korea	Spring/2011	TSP	3.0		25	*(Kirillova et al., 2014a)*
Average						33±14	
South Asia							
Background	Hainan, China	Annual 2005/2006	$PM_{2.5}$	3.9	0.54	18	(Zhang et al., 2014b)
Background	Hainan, China	Winter 2005/2006	$PM_{2.5}$	6.2	0.57	14.5	(Zhang et al., 2014b)
Background	Hainan, China	Summer 2005/2006	$PM_{2.5}$	1.4	0.40	17.7	(Zhang et al., 2014b)
Background	Hanimaadhoo, Maldives	Annual 2008/2009	TSP	0.5		17	(Kirillova et al., 2013)
Background	Sinhagad, India	Annual 2008/2009	TSP	3.0		24	(Kirillova et al., 2013)
Background	Hanimaadhoo, Maldives	Spring/2012	$PM_{2.5}$	0.6	0.62	14	(Bosch et al., 2014)
Urban	Delhi, India	Winter/2010/ 2011	$PM_{2.5}$	22.0		21	(Kirillova et al., 2014b)
Average						18±4	

Europe and USA							
Urban	Göteborg, Sweden	Winter/2005	$PM_{2.5}$	1.1	0.48	23	(Szidat et al., 2009)
Urban	Göteborg, Sweden	Summer/2006	$PM_{2.5}$	0.8	0.61	30	(Szidat et al., 2009)
Rural	Göteborg, Sweden	Winter/2005		1.2	0.53	27	(Szidat et al., 2009)
Rural/semi-urban	Stockholm, Sweden	Summer/2009	TSP			12	(Kirillova et al., 2010)
Urban	Zürich, Switzerland	Summer/2002	PM_{10}	2.1	0.54	14	(Szidat et al., 2004)
Urban	Zürich, Switzerland	Winter/2008	PM_{10}	2.8	0.60	26.8	(Zhang et al., 2013)
Urban	Moleno, Switzerland	Summer/2006	PM_{10}	5.3	0.67	30	(Zhang et al., 2013)
Urban	Bern, Switzerland	Winter/2009	PM_{10}		0.39	14	(Zhang et al., 2014c)
Urban	Atlanta, USA	Summer/2004	$PM_{2.5}$	2.3	0.59	26.5	(Weber et al., 2007)
Rural	Millbrook, USA	Annual/2006/2007	TSP		0.36	12	(Wozniak et al., 2012)
Rural	Harcum, USA	Annual/2006/2007	TSP		0.38	14	(Wozniak et al., 2012)
Regional background	Cesar, Netherlands	Annual/2011/2012	$PM_{2.5}$	2.3	0.65	21	(Dusek et al., 2017)
Average						21±8	

639

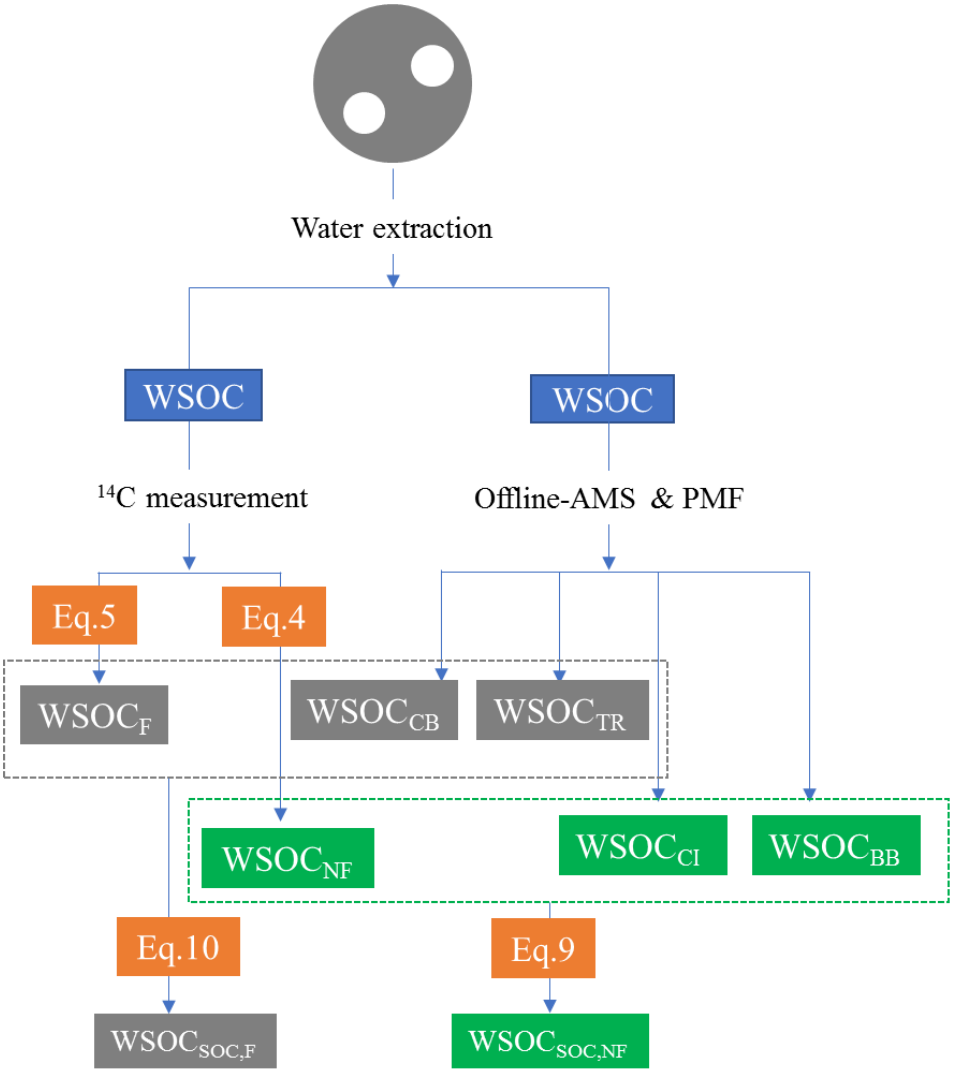

640

641 **Figure 1**. The AMS[2]-based source apportionment scheme of WSOC aerosols in this study.

642 See the main text for the equations (i.e., Eq. 4, 5, 9, 10 in the Sec. 2.5) and the offline-AMS &

643 PMF (see the Sec. 2.3).

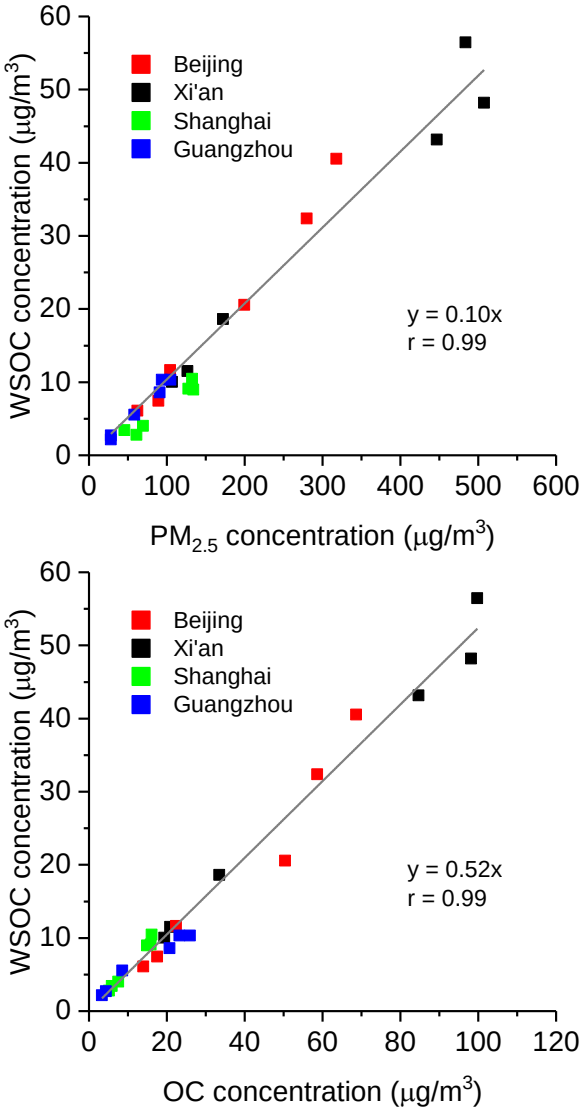

644

645 **Figure 2**. Linear relationships ($p<0.01$) of WSOC with $PM_{2.5}$ (top) and OC concentrations

646 (bottom).

647

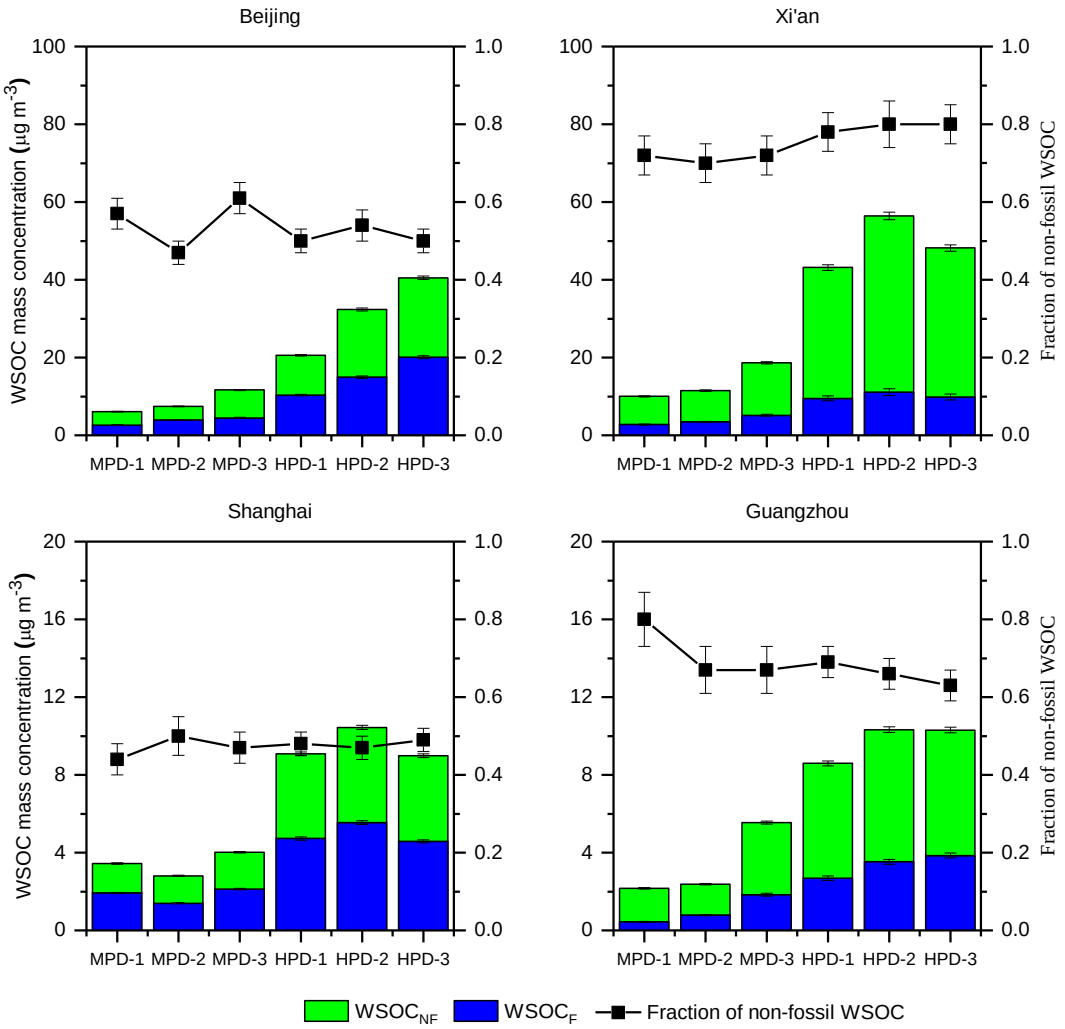

Figure 3. Mass concentrations (μg/m^3) of WSOC from non-fossil and fossil-fuel sources ($WSOC_{NF}$ and $WSOC_F$, respectively) as well as non-fossil fractions of the WSOC aerosols from Beijing, Xi'an, Shanghai and Guangzhou during moderately polluted days (MPD) and heavily polluted days (HPD). Note the different scaling for different cities.

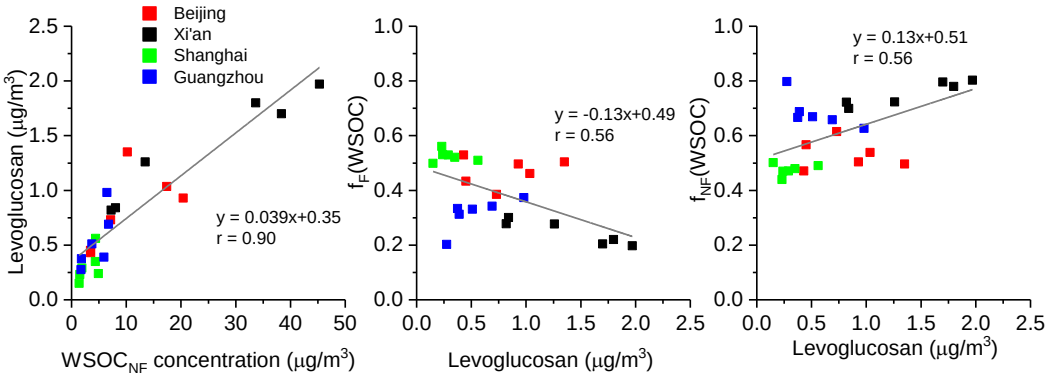

654

655 **Figure 4.** Relationships of non-fossil derived WSOC ($WSOC_{NF}$) and levoglucosan (left),

656 levoglucosan and fraction of fossil to WSOC (f_F(WSOC)) (middle) and levoglucosan and

657 fraction of non-fossil to WSOC (f_{NF}(WSOC)) (right).

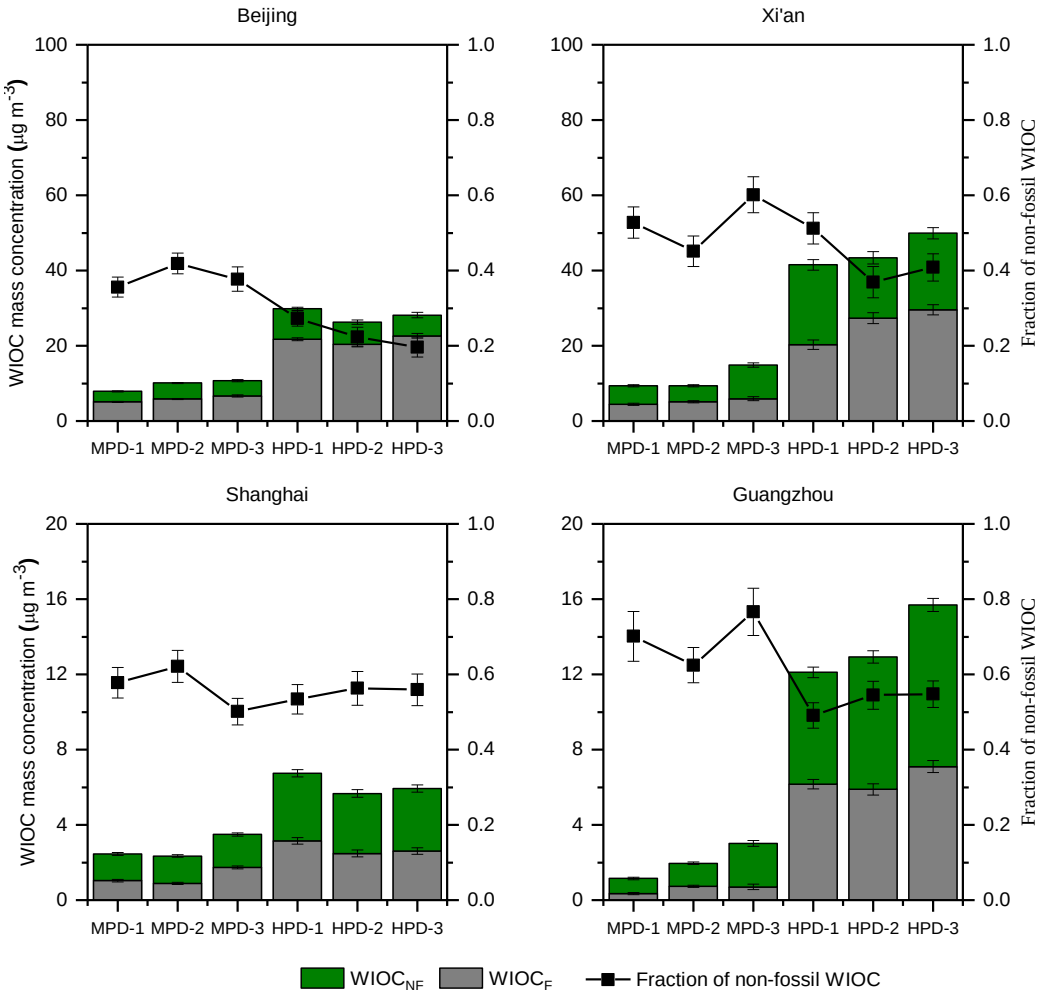

658

659 **Figure 5**. Mass concentrations (μg/m^3) of WIOC from non-fossil and fossil-fuel sources
660 (WIOC $_{NF}$ and WIOC $_{F}$, respectively) as well as non-fossil fractions in the WIOC aerosols from
661 Beijing, Xi'an, Shanghai and Guangzhou during moderately polluted days (MPD) and heavily
662 polluted days (HPD). Note the different scaling for different cities.

663

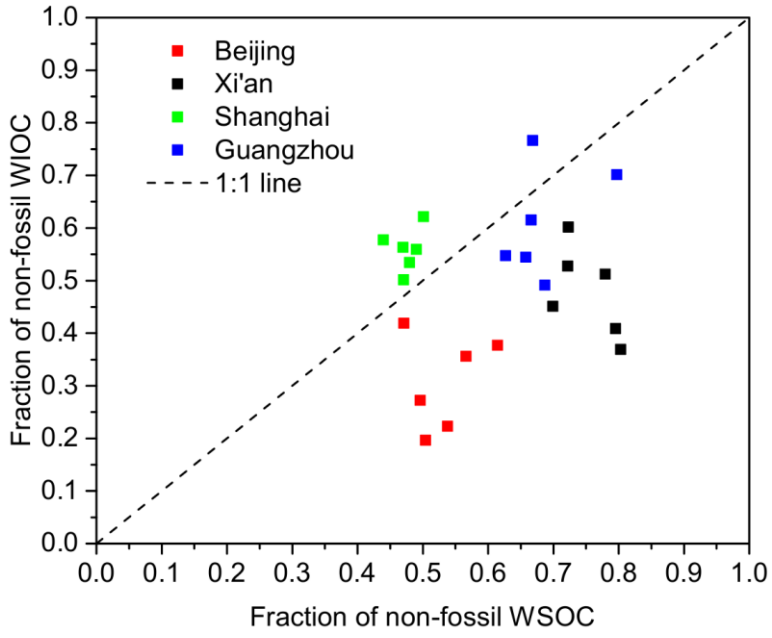

664

665 **(a)**

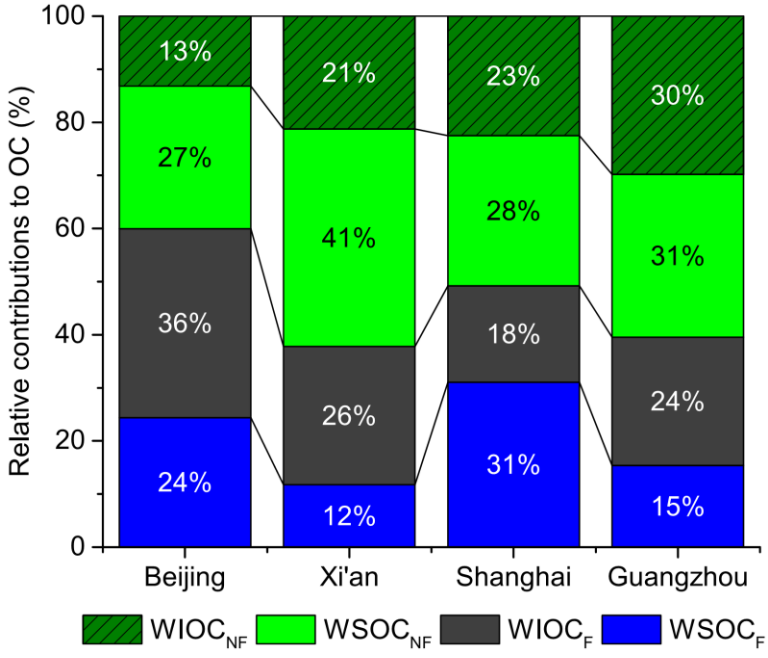

666

667 **(b)**

668 **Figure 6**. Relationship between the fraction of non-fossil WIOC and WSOC(a) and averaged

669 relative contribution (%) to OC from WSOC and WIOC from non-fossil and fossil sources (b).

670

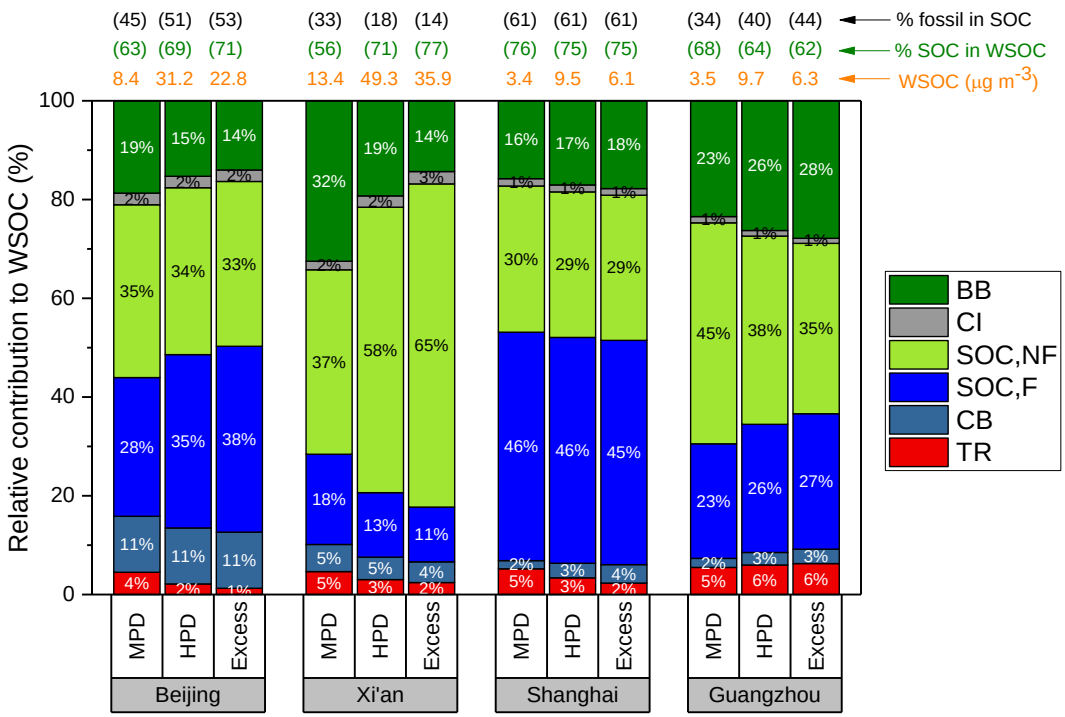

671

672 **Figure 7.** Relative contributions (%) to WSOC from biomass burning as well as secondary
673 organic carbon (SOC) from fossil and non-fossil sources ($WSOC_{SOC,F}$ and $WSOC_{SOC,NF}$,
674 respectively) in different cities during moderately polluted days (MPD) and heavily polluted
675 days (HPD) as well as their corresponding excess (Excess=HPD-MPD). The numbers above
676 the bars refer to the average WSOC concentrations and the SOC fractions (%) of WSOC.

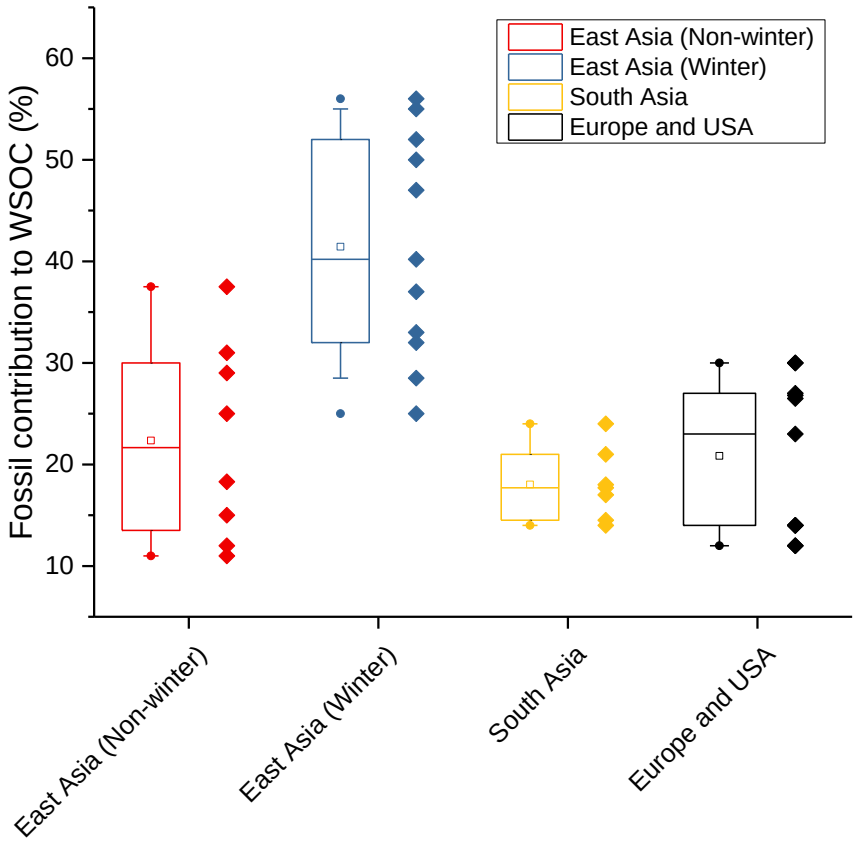

677

678 **Figure 8.** Box-plot of the fossil contribution (%) to the WSOC aerosols in East Asia, South
679 Asia, USA and Europe. The box represents the 25th (lower line), 50th (middle line) and 75th (top
680 line) percentiles; the empty square within the box represent the mean values; the end lines of
681 the vertical bars represent the 10th (below the box) and 90th (above the box) percentiles; the
682 solid dots represents the maximum and minimum values; the solid diamonds represent the
683 individual data (Table 1). The data from East Asia is grouped by the winter and non-winter
684 seasons.